Voltage Collapse Margin Sensitivity Methods applied to the Power System of Southwest England

Scott Greene   **Ian Dobson**

Electrical & Computer Engineering Department
University of Wisconsin-Madison
1415 Engineering Drive
Madison WI 53706 USA
phone (608) 262 2661
fax (608) 262 1267
email dobson@engr.wisc.edu

February 18, 1998

Contents

List of Figures

List of Tables

Chapter 1

Introduction

1.1 Summary

This report applies sensitivity methods to a model of the Southwest of England electric power system to determine their effectiveness in operating the system sufficiently far from voltage collapse blackouts. The sensitivity methods were developed at the University of Wisconsin and are described in detail in [12, 13]. The system data was graciously provided by the National Grid Company.

The two main uses of the sensitivity methods are

1. Quickly quantify the effect of varying power system controls or parameters on the proximity to voltage collapse

2. Quickly rank the severity of contingencies with respect to voltage collapse

The results confirm that the sensitivity methods perform well on the Southwest of England model for these uses.

The Southwest of England model used in this report has 40 buses. We anticipate no difficulty in applying the sensitivity methods to systems represented with more buses; the largest model we have tested was a 1390 bus model in [13]. In this report, the only system change considered as load increased was generator VAR limits. We believe that changes in other devices and operator actions as load is increased could be handled with our methods

as long as the underlying continuation method took proper account of these effects.

The report also examines the effect of generator VAR limits and presents a sensitivity computation for cases in which instability is directly precipitated by a VAR limit. However, we found no cases in which the loading margin error in neglecting the instabilities precipitated by the VAR limit exceeded 11 MW.

The results were obtained using software developed at the University of Wisconsin. The hardest part of the computation is locating the voltage collapse as load is increased; the sensitivity computations themselves are quick and relatively simple. The National Grid Company has software to locate voltage collapse [14] and our impression is that this software could readily be modified to additionally perform the sensitivity computations described in this report. We suggest that the National Grid Company consider this modification. It would be interesting to explore the possibility of including the margin sensitivity computations from this report with the on-line power management methods described in [14].

We invite comments from the National Grid Company staff about the advantages and limitations of the sensitivity methods for the National Grid Company power system. Such feedback is very valuable in directing research at the University of Wisconsin along productive lines.

1.2   Background

Voltage collapse is an instability of heavily loaded electric power systems characterized by monotonically decreasing voltages and blackout [5, 3, 4]. Secure operation of a power system requires appropriate planning and control actions to avoid voltage collapse.

For a particular operating point, the amount of additional load in a specific pattern of load increase that would cause a voltage collapse is called the loading margin. Loading margin is an accurate measure of proximity to voltage collapse which takes account of system limits and nonlinearities. (Every paper on other voltage collapse indices implicitly acknowledges the

significance of loading margin by using it as the horizontal scale when the performance of the proposed index is graphed.) The loading margin can be found by computing a continuation of equilibrium solutions corresponding to increasing loads. We are interested in how the loading margin of a power system changes as system parameters or controls are altered.

This report describes computing and exploiting the sensitivity of the loading margin to voltage collapse with respect to various parameters. The main idea of this report is that after the loading margin has been computed for nominal parameters, the effect on the loading margin of altering the parameters can be predicted by Taylor series estimates. The linear Taylor series estimates are extremely quick and easy and allow many variations on the nominal case to be quickly explored. Exhaustively recomputing the point of voltage collapse instability for each parameter change is avoided. For more details and a review of previous work see [12, 13]. [12] describes the use of loading margin sensitivities with respect to general parameter and controls while [13] describes the use of loading margin sensitivities to quickly rank the severity of contingencies.

Chapter 2

Nominal Voltage Collapse Margin

2.1 Computing the nominal voltage collapse

The nominal point of voltage collapse is the theoretical limit of the steady state model of the power system and is not a reasonable point at which to operate the actual power system. However, by computing the nominal point of collapse, and thus the loading margin to collapse, one can assess the security of the actual system operated at a nominal stable operating point. In addition, the effects of contingencies and events on the security of the actual system can be analysed by computing the effects of the contingencies and events on the loading margin to collapse.

The test system consists of 40 buses representing a portion of the South West Peninsula power grid and is described in [15]. For this study, transformer taps and switched compensation devices were assumed fixed.

The derivations and application of the sensitivity formulas [12] require the choice of a nominal stable operating point at which parameters or controls are to be adjusted, and a projected pattern of load increase. The nominal stable operating point is shown in Table 2.1. Bus types are differentiated as:

- 'PQ', bus voltage and angle vary to maintain specified real and reactive power injections.

- 'PV', reactive power output and bus angle vary to maintain specified real power injection and voltage.

- 'VA', real and reactive power output vary to maintain specified bus voltage and angle.

The pattern of load increase is a direction in loading space along which the loading margin is measured. The direction of load increase is shown in Table 2.3. Note that the sum of the real power components of the load direction is unity. Thus the direction of load increase is a unit vector using the L^1 norm.

The nominal point of collapse must be computed by a method that takes into account system limits such as generator reactive power limits as they are encountered. In general, the limits enforced at the point of collapse are different than those at the stable operating point.

The nominal voltage collapse was established as follows: From the base case equilibrium point (Table 2.1) representing a total load of 3575 MW, the loading was gradually increased at the specified buses in the proportions shown in Table 2.3. The effect of generators reaching VAR limits listed in Table 2.2 was modeled by replacing 'PV' buses with 'PQ' buses at the loading at which VAR limits were reached. Transformer taps were held fixed at the starting ratios. No other changes to the network parameters were implemented. In particular, no shunts were adjusted as the loading was increased. The base case system encountered a voltage collapse at a total load of 5380 MW, and thus the nominal margin is 1805 MW. Prior to voltage collapse, the PV buses at EXET0, FAWL0, and LOVE0 encountered VAR limits, and the PV bus at HINP0 was very close to reaching its VAR limit. Table 2.4 shows the solution at the nominal point of collapse. Generators that have reached reactive power limits are indicated in **bold face** as is the VAR output at HINP0 which is precariously close to a VAR limit.

The Jacobian of the equilibrium equations with respect to the state variables at the nominal point of collapse is singular (fold bifurcation). The left eigenvector corresponding to the zero eigenvalue of the system Jacobian matrix evaluated at the nominal point of collapse is shown in Table 2.5, normalized so that the largest component is unity. This left eigenvector is the normal vector to the set of real and reactive power injections that correspond to a fold bifurcation of the equilibrium equations [Dobson,Greene1]. The left eigenvector indicates that the bus with the greatest influence on the loading margin is the Indian Queens 132kV bus.

Table 2.1: Nominal stable operating point

Bus	Bus	Bus	Voltage	Angle	Load		Generation	
No.	Name	Type	(p.u.)	(degrees)	(MW)	(VAR)	(MW)	(VAR)
1	INDQ4	PQ	1.014	-1.437	-	-	-	-
2	LAND4	PQ	1.007	-1.648	-	-	-	-
3	ABHA4T	PQ	1.011	-0.852	-	-	-	-
4	ABHA4U	PQ	1.008	-1.097	-	-	-	-
5	EXET4	PQ	1.016	-0.142	-	-	-	-
6	EXET0	PV	1.020	-0.142	-	-	-	12.9
7	TAUN4J	PQ	1.016	0.956	-	-	-	-
8	TAUN4K	PQ	1.018	0.865	-	-	-	-
9	AXMI4	PQ	1.014	-0.317	-	-	-	-
10	CHIC4	PQ	1.013	-0.201	-	-	-	-
11	MANN4	PQ	1.008	-0.033	-	-	-	-
12	LOVE4	PQ	1.006	0.721	422.0	-63.8	-	-
13	LOVE0	PV	1.010	0.721	-	-	-	11.1
14	NURS4	PQ	1.005	1.212	200.4	48.4	-	-
15	FLEE4	PQ	1.006	-0.416	469.1	96.5	-	-60.0
16	BRLE4	PQ	1.009	-0.478	-	-	-108.8	86.3
17	HINP4	PQ	1.014	2.109	-	-	-	-
18	HINP0	PV	1.000	8.683	-	-	1099.1	-77.7
19	HINP2J	PQ	0.994	3.476	-	-	-	-
20	HINP0J	PV	1.000	13.140	-	-	207.8	19.6
21	HINP2K	PQ	0.994	3.488	-	-	-	-
22	HINP0K	PV	1.000	13.153	-	-	207.8	19.7
23	MELK4	PQ	1.015	-0.140	-	-	-392.6	42.5
24	DIDC4	PV	1.005	-0.541	-	-	-38.6	-177.0
25	BOLN4	PQ	0.998	0.573	518.5	117.3	-	-
26	NINF4	PQ	0.994	1.710	358.4	153.1	-	-
27	BRWA2Q	PQ	0.987	3.036	-	-	-	-
28	BRWA2R	PQ	0.987	3.054	-	-	-	-
29	INDQ1	PQ	0.898	-8.621	294.8	63.7	-	-
30	LAND1	PQ	0.969	-5.284	131.6	39.1	-	-
31	ABHA1	PQ	0.984	-4.412	157.9	46.9	-	-
32	EXET1	PQ	0.951	-3.881	142.2	22.4	-	-
33	CHIC1	PQ	0.956	-1.228	40.0	5.6	-	-
34	MANN1	PQ	0.960	-4.609	368.5	91.6	-	-
35	AXMI1	PQ	0.967	-2.289	84.2	22.4	-	-
36	TAUN1	PQ	0.962	-1.860	31.6	6.7	-	-
37	BRWA1	PQ	0.992	-1.658	200.1	-	-	-
38	FAWL4	PQ	1.005	1.841	156.0	57.4	-	-
39	FAWL0	PV	1.000	8.420	-	-	1806.5	-9.5
40	DUNG4	VA	0.996	3.400	-	-	819.1	-26.4

Table 2.2: Reactive power limits

Bus No.	Bus Name	Maximum (VAR)	Minimum (VAR)
6	EXET0	150	-75
13	LOVE0	150	-75
18	HINP0	660	-9999
20	HINP0J	150	-9999
22	HINP0K	150	-90
24	DIDC4	9999	-9999
39	FAWL0	470	-9999

Table 2.3: Direction of load increase

Bus No.	Bus Name	Real Power	Reactive Power
29	INDQ1	0.2032	0.0439
30	LAND1	0.0907	0.0270
31	ABHA1	0.1089	0.0324
32	EXET1	0.0980	0.0154
33	CHIC1	0.0276	0.0039
34	MANN1	0.2540	0.0632
35	AXMI1	0.0581	0.0154
36	TAUN1	0.0218	0.0046
37	BRWA1	0.1379	0.0000

Table 2.4: Nominal point of collapse

Bus No.	Bus Name	Bus Type	Voltage (p.u.)	Angle (degrees)	Load (MW)	(VAR)	Generation (MW)	(VAR)
1	INDQ4	PQ	0.832	-29.32	-	-	-	-
2	LAND4	PQ	0.826	-29.88	-	-	-	-
3	ABHA4T	PQ	0.863	-27.28	-	-	-	-
4	ABHA4U	PQ	0.851	-28.03	-	-	-	-
5	EXET4	PQ	0.895	-25.03	-	-	-	-
6	**EXET0**	**PQ**	0.948	-25.03	-	-	-	150.0
7	TAUN4J	PQ	0.914	-23.43	-	-	-	-
8	TAUN4K	PQ	0.915	-23.71	-	-	-	-
9	AXMI4	PQ	0.899	-24.20	-	-	-	-
10	CHIC4	PQ	0.907	-22.47	-	-	-	-
11	MANN4	PQ	0.916	-20.09	-	-	-	-
12	LOVE4	PQ	0.958	-14.54	422.0	-63.8	-	-
13	**LOVE0**	**PQ**	1.008	-14.54	-	-	-	150.0
14	NURS4	PQ	0.957	-14.44	200.4	48.4	-	-
15	FLEE4	PQ	0.972	-17.45	469.1	96.5	-	-60.0
16	BRLE4	PQ	0.982	-18.12	-	-	-108.8	86.3
17	HINP4	PQ	0.937	-21.56	-	-	-	-
18	**HINP0**	PV	1.000	-14.50	-	-	1099.1	**650.0**
19	HINP2J	PQ	0.924	-21.67	-	-	-	-
20	HINP0J	PV	1.000	-11.38	-	-	207.8	107.7
21	HINP2K	PQ	0.924	-21.65	-	-	-	-
22	HINP0K	PV	1.000	-11.35	-	-	207.8	107.6
23	MELK4	PQ	0.963	-20.77	-	-	-392.6	42.5
24	DIDC4	PV	1.005	-18.30	-	-	-38.6	582.1
25	BOLN4	PQ	0.958	-8.433	518.5	117.3	-	-
26	NINF4	PQ	0.971	-2.317	358.4	153.1	-	-
27	BRWA2Q	PQ	0.912	-22.70	-	-	-	-
28	BRWA2R	PQ	0.912	-22.66	-	-	-	-
29	INDQ1	PQ	0.569	-61.26	661.6	142.9	-	-
30	LAND1	PQ	0.717	-43.48	295.4	87.8	-	-
31	ABHA1	PQ	0.786	-39.44	354.4	105.3	-	-
32	EXET1	PQ	0.787	-37.56	319.0	50.2	-	-
33	CHIC1	PQ	0.852	-25.36	89.8	12.5	-	-
34	MANN1	PQ	0.821	-33.42	827.0	205.7	-	-
35	AXMI1	PQ	0.839	-29.97	189.0	50.2	-	-
36	TAUN1	PQ	0.845	-33.64	70.9	15.1	-	-
37	BRWA1	PQ	0.883	-34.07	449.0	-	-	-
38	FAWL4	PQ	0.957	-13.97	156.0	57.4	-	-
39	**FAWL0**	**PQ**	0.983	-6.965	-	-	1806.5	470.0
40	DUNG4	AV	0.996	3.400	-	-	2748.7	601.2

Table 2.5: Left eigenvector corresponding to the zero eigenvalue of the system Jacobian at the nominal point of collapse.

Bus No.	Bus Name	Real Power	Reactive Power
1	INDQ4	0.1172	0.3041
2	LAND4	0.1227	0.2936
3	ABHA4T	0.0899	0.2240
4	ABHA4U	0.0984	0.2386
5	EXET4	0.0683	0.1710
6	EXET0	0.0683	0.1530
7	TAUN4J	0.0552	0.1439
8	TAUN4K	0.0568	0.1445
9	AXMI4	0.0625	0.1545
10	CHIC4	0.0522	0.1337
11	MANN4	0.0404	0.1056
12	LOVE4	0.0206	0.0542
13	LOVE0	0.0206	0.0491
14	NURS4	0.0207	0.0593
15	FLEE4	0.0238	0.0373
16	BRLE4	0.0242	0.0307
17	HINP4	0.0421	0.1031
18	HINP0	0.0281	0.0000
19	HINP2J	0.0450	0.0916
20	HINP0J	0.0258	0.0000
21	HINP2K	0.0449	0.0915
22	HINP0K	0.0257	0.0000
23	MELK4	0.0341	0.0651
24	DIDC4	0.0221	0.0000
25	BOLN4	0.0094	0.0337
26	NINF4	0.0027	0.0157
27	BRWA2Q	0.0502	0.0967
28	BRWA2R	0.0500	0.0966
29	INDQ1	0.9086	1.0000
30	LAND1	0.3177	0.4820
31	ABHA1	0.2107	0.3091
32	EXET1	0.1730	0.2479
33	CHIC1	0.0660	0.1364
34	MANN1	0.0988	0.1357
35	AXMI1	0.0955	0.1670
36	TAUN1	0.1122	0.1572
37	BRWA1	0.1085	0.1385
38	FAWL4	0.0198	0.0617
39	FAWL0	0.0048	0.0597
40	DUNG4	0.0000	0.0000

Chapter 3

Loading Margin Sensitivity

3.1   Introduction

This chapter describes and illustrates the use of loading margin sensitivities to avoid voltage collapse. The nominal stable operating point and the nominal point of collapse are described in chapter 2.

The derivation of the sensitivity formulas assumes that the system equations remain fixed as parameters are varied. In particular, the limits enforced at the point of collapse are assumed to stay the same as parameters are varied. (A change in the system limits corresponds to a change in the system equations and the sensitivity based estimates using the equations valid at the nominal nose can become inaccurate when the parameters change sufficiently so that the equations change.)

For this study, when a generator represented by a 'PV' bus reaches a reactive power limit, it is converted to a 'PQ' bus, effectively changing the equilibrium equations modeling the system. In [12] and [13], the major cause for inaccuracies of the sensitivity based estimates is shown to be generator reactive power limits changing as parameters are varied.

The case studied here is challenging since the generator at HINP0 is very close to a limit at the nominal point of collapse. It is likely that for changes in some parameters, the maximum VAR limit at HINP0 will be reached prior to the new collapse point.

3.2 Computation of linear sensitivity

The linear estimate of the change in loading margin (ΔL) resulting from a change to an arbitrary parameter (Δp) is:

$$\Delta L = L_p \Delta p = \frac{-w F_p \Delta p}{w F_\lambda \hat{k}} \tag{3.1}$$

where :

- L_p is the sensitivity of the loading margin with respect to the parameter.

- F, are the power system equilibrium equations (real and reactive power balance at each bus) that apply at the nose. In particular, F accounts for the power system limits enforced at the nose.

- F_λ, the derivative of F with respect to the load parameters. For constant power load models F_λ is a diagonal matrix with ones in the rows corresponding to buses with loads.

- F_p, the derivative of the equilibrium equations with respect to the parameter p at the nominal nose point. The parameter can be a vector and then F_p is a matrix.

- w, the left eigenvector corresponding to the zero eigenvalue of the system Jacobian F_x (F_x evaluated at a fold bifurcation is singular).

- $\hat{k}$, the unit vector in the direction of load increase. $\hat{k}$ also defines the direction in which the loading margin is measured. The direction of load increase is shown in Table 2.3.

The denominator of (3.1) is a scaling factor that is the same for all parameter changes. The linear sensitivity can be improved with a quadratic estimate, derived and explained in [12].

3.3 Sensitivity with respect to load variation

Table 2.5 shows the left eigenvector corresponding to the zero eigenvalue of the system Jacobian evaluated at the nominal fold point. This left eigenvector

14

indicates that the voltage collapse is most affected by the load at the 132 KV Indian Queens bus. There are several situations in which the sensitivity of the margin to voltage collapse with respect to the load would be of interest.

There is usually uncertainty in the metering or forecast of loads. By computing the sensitivity to the load, one can estimate the effects of inaccuracy in the nominal values used. Secondly, it might be possible to shed load at a bus, and it would be useful to know how much margin can be gained for each MW of load shed. Finally, the sensitivity computation identifies buses that are good candidates for planned improvements. For example, load margin sensitivity can specify good locations for VAR support or areas where interruptible contracts would contribute the most to system security.

Methods

The loading margin corresponding to various loads of the same power factor at the 132KV Indian Queens Bus is computed by the same continuation method used to obtain the nominal fold bifurcation. The results are compared to those obtained using the linear sensitivity formulas evaluated at the nominal fold bifurcation.

There is 294 MW of 0.98 power factor load at the Indian Queens 132KV bus at the nominal stable operating point. Results are obtained for a variation of ± 50MW, which is $\pm 17\%$ of the base load.

Results

The solid lines in Figures 3.1 and 3.2 are the linear estimates for the loading margin variation as a function of the load shed. The dots in Figures 3.1 and 3.2 represent the actual values of the loading margin as computed by the continuation method.

Figure 3.1 shows the effects on the loading margin for increasing the load at INDQ0 by 10 MW increments at power factor 0.98. The dots represent the collapse points as computed by continuation, and the line represents the linear estimate. Figure 3.2 shows the effects on the loading margin for decreasing the load at INDQ0 by 10 MW increments at power factor of 0.98.

The agreement between the linear estimates and the actual margins is excellent over the entire range, but better for the increase in load than the reduction of load. Closer inspection showed that a reduction of any more than

3 MW caused the generator at HINP0 to reach its reactive power limit prior to voltage collapse. The nearby VAR limit at HINPO affected the accuracy of the estimates as expected. Although the effect is recognizable as a deviation from the linear estimate, the magnitude of the error is insignificant. (In fact, the HINP0 VAR limit causes an immediate instability (see Chapter 5). The immediate instability occurs before the fold point and is shown by the circles in Figure 3.3.)

3.4   Sensitivity with respect to VAR limits

Computation of the nominal voltage collapse point showed that Buses EXET0, FAWL0, and LOVE0 all encounter VAR limits. We find out from sensitivities how the loading margin to voltage collapse would change if these limits were different.

Methods

The magnitude of the components of the left eigenvector (Table 2.5) corresponding to reactive power injections indicates that of the three generators that encounter VAR limits between the nominal stable operating point and the point of collapse, the generator at the 132 KV bus at Exeter has the greatest influence on the margin to collapse. The loading margin corresponding to various maximum reactive power limits at the 132KV Exeter bus is computed by the same continuation method used to obtain the nominal fold bifurcation. The results are compared to those obtained using the linear sensitivity formula evaluated at the nominal fold bifurcation.

The nominal maximum reactive power limit at the Exeter 132KV bus is 150 MVARs. Results are obtained for a variation of 30 MVARs, which is $\pm 20\%$ of the nominal reactive loading.

Results

The solid lines in Figure 3.4 shows the linear estimate for the loading margin variation as a function of the maximum reactive power limit at the 132 KV Exeter bus. The dots in Figure 3.4 represent the actual values of the loading

Figure 3.1: Effect of load increase at Indian Queens on the loading margin to voltage collapse
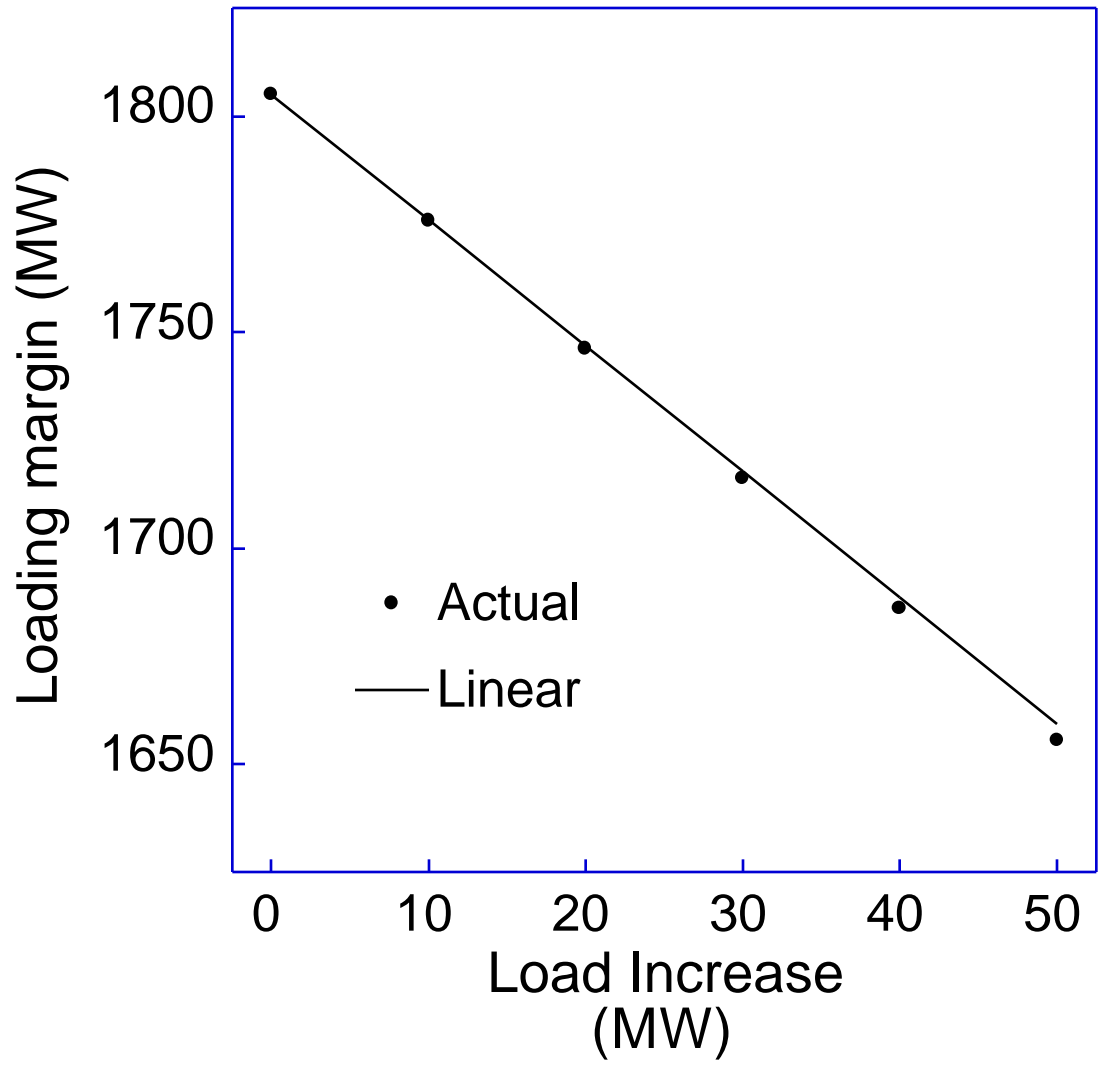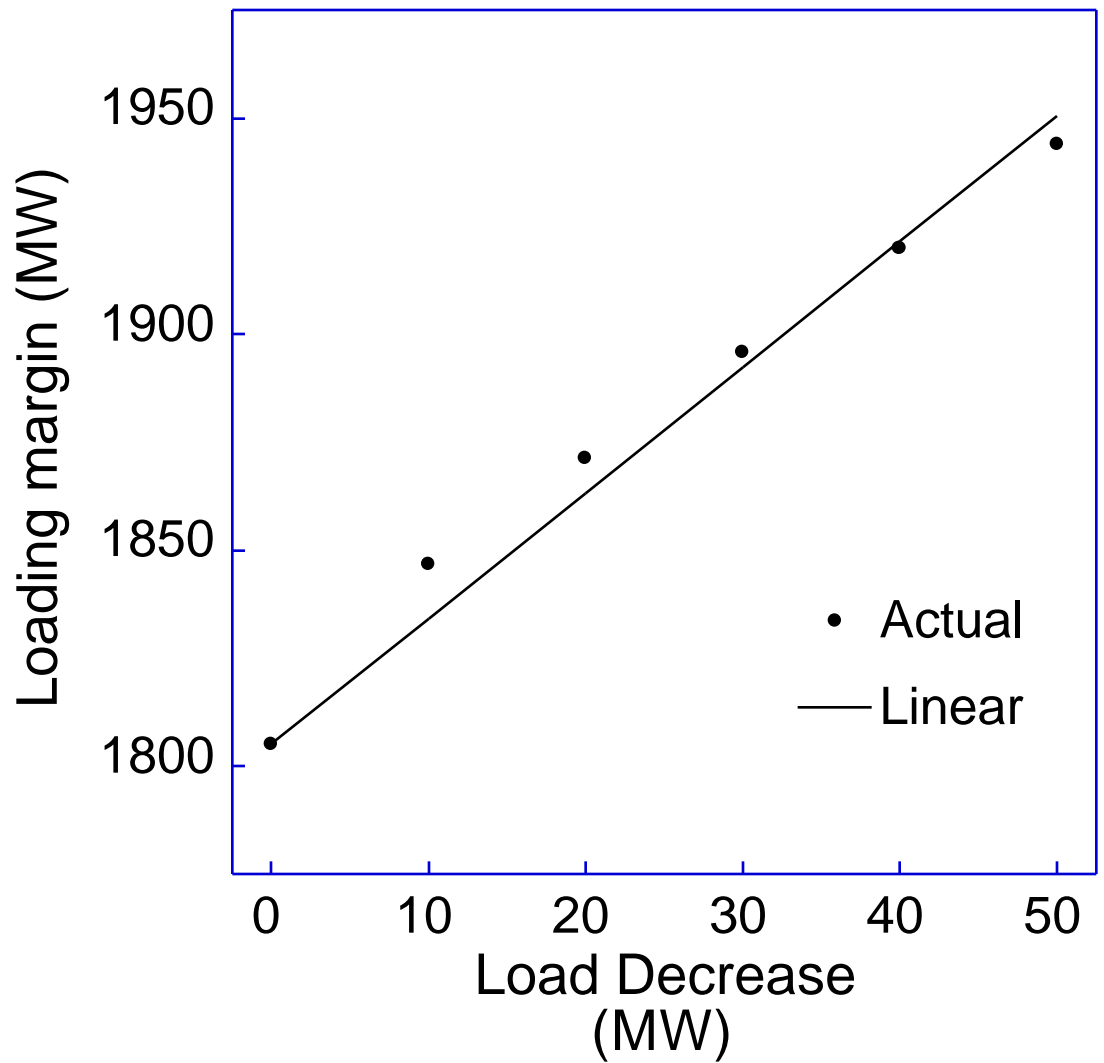
Figure 3.2: Effect of load decrease at Indian Queens on the loading margin to voltage collapse
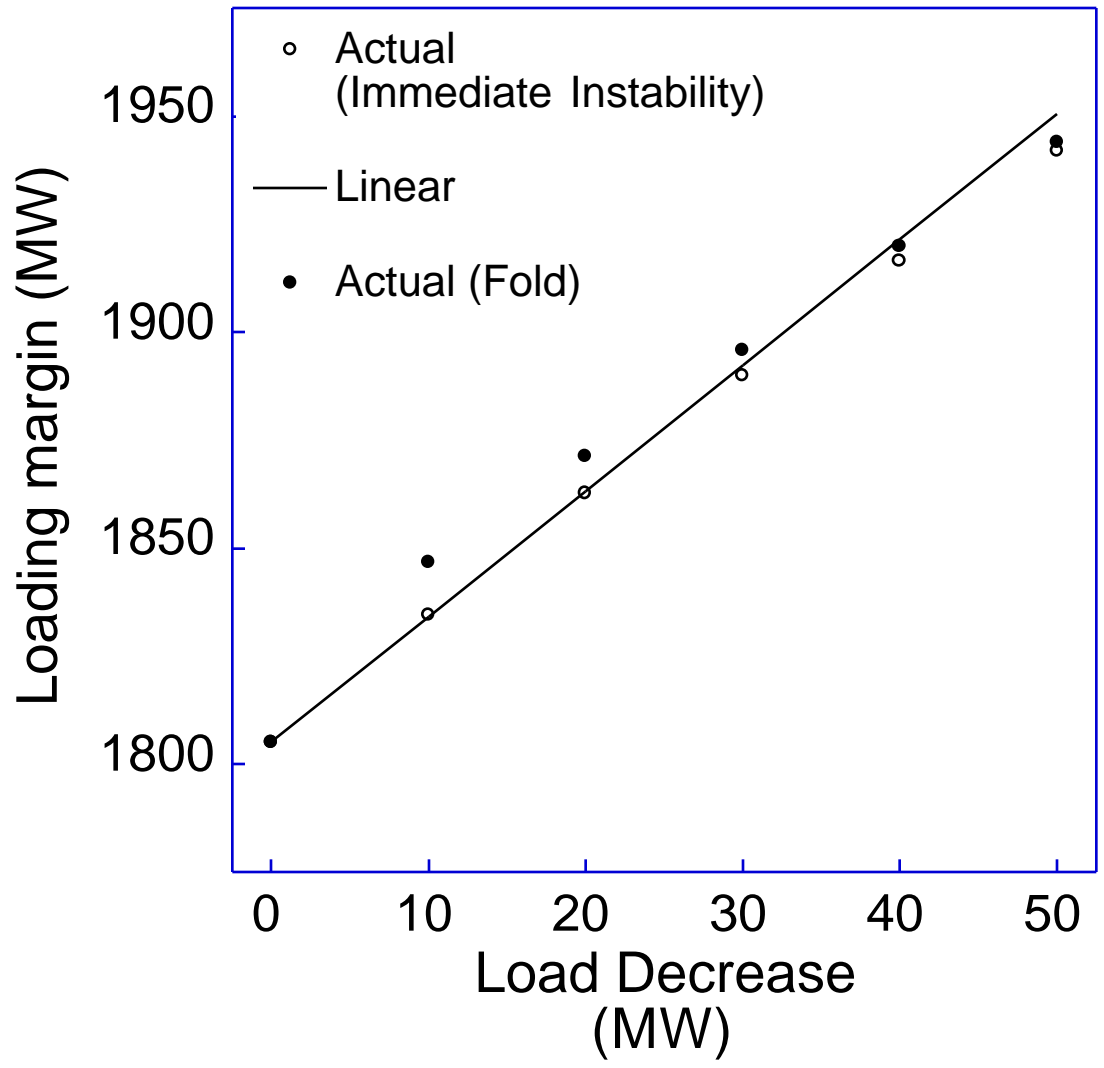
Figure 3.3: Effect of load decrease at Indian Queens on the loading margin to voltage collapse and critical VAR limit

margin as computed by the continuation method. The agreement between the linear estimates and the actual margins is excellent over the entire range.
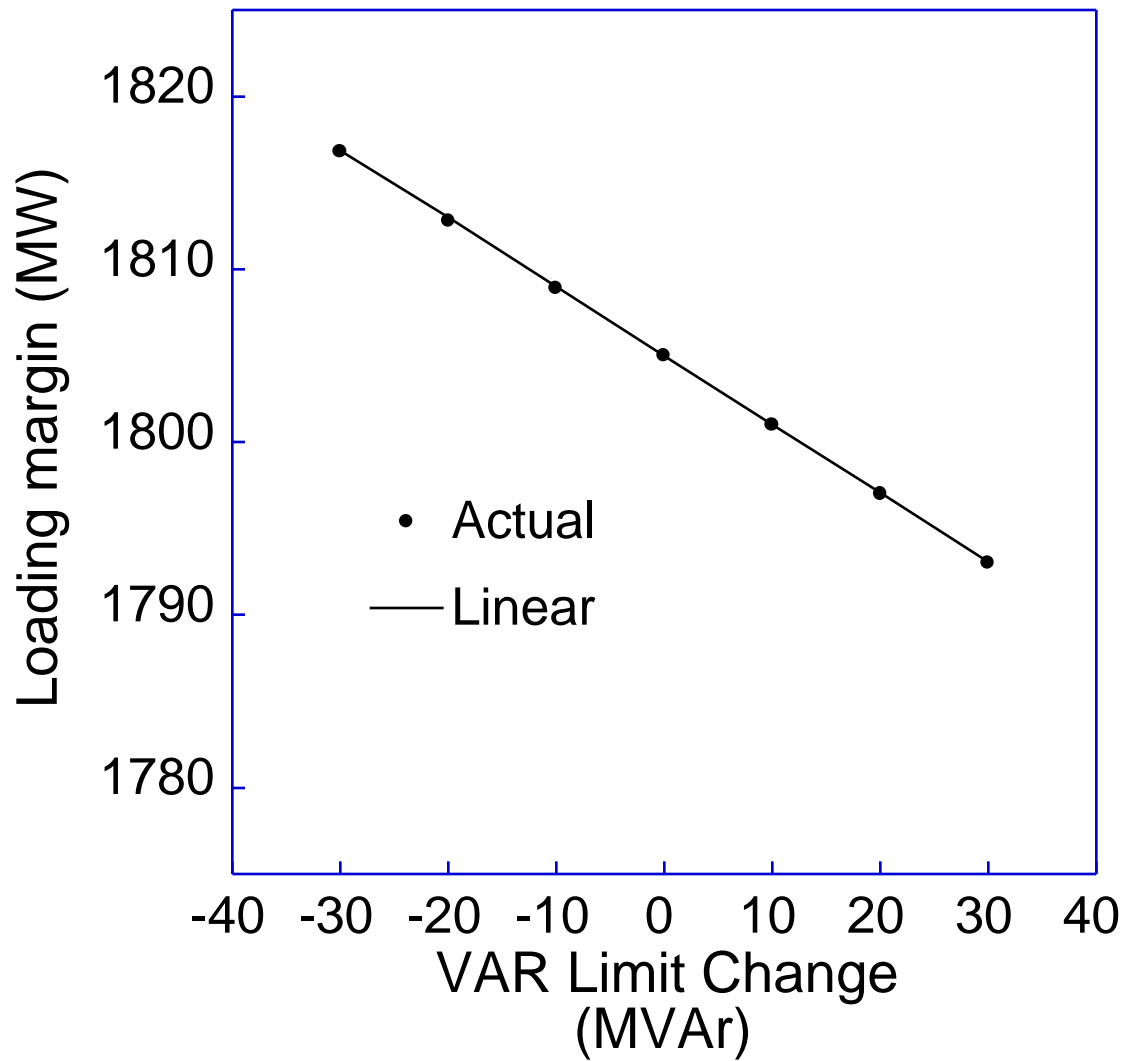
Figure 3.4: Effect of variation in VAR limit at Exeter on the loading margin to voltage collapse

Chapter 4

Contingency Ranking for Voltage Collapse

The sensitivity formulas of the previous chapter can be used to rank the effects of contingencies on the margin to voltage collapse. In this case the parameter p is a vector representing the line admittance, and instead of looking at the effect of small deviations, the admittance parameter is changed from its nominal value to zero.

4.1   Method

The estimates for the effects of contingencies were computed as described in [13]. The actual margins resulting from the contingencies were computed by first identifying a stable post contingency equilibrium at the base case loading and then gradually increasing the load and accounting for VAR limits until a voltage collapse due to fold bifurcation of the equilibrium equations was found.

Radial line outages are a special case in which the derived formulas do not strictly apply since the post outage network will not be connected. We suggest that the contingency list be first screened to identify radial lines, and that these outages be analysed and ranked separately from the other contingencies. [1]

---

[1]For the system used for this report, all radial line outages result in isolation of a single bus. The estimates were then obtained by assuming a reduced system in which

4.2   Results

Table 4.1 compares the estimates to the actual margins for all non-radial line outages resulting in at least a 75 MW reduction in loading margin. The ranks correspond to the rank of each outage among all other non-radial line outages. Table 4.2 compares the estimates to the actual margins for all radial line outages, with ranking shown among only radial lines. The two most critical radial line outages are among the most critical line outages and are identified as so. However, the estimates for the radial line outages tend to be better than the estimates for non-radial outages, and so the moderate radial outages tend to be ranked too high when included with all line outages. Table 4.3 shows the remaining line outages. Outages mis-grouped by the estimates are shown in bold face. The radial outages were all ranked correctly.

For the four outages causing less than a 10 MW change in margin, the mean error for the linear estimate was 3.0 MW and the maximum error was 4 MW. For the ten outages causing between a 10 MW and 20 MW change in margin, the mean error was 3.9 MW and the maximum error was 13 MW. For the thirteen outages causing between a 20 MW and 45 MW change in margin, the mean error was 10.4 MW and the maximum error was 26 MW. The estimates captured the thirteen worst non-radial line outages, all causing greater than 60 MW change in the margin. The worst results pertained to the outages between BRWA2Q and HINP2J (27.19.1) and BRWA2R and HINP2K (28.21.1).

As noted in [13], the major cause for inaccuracy was due to changes in the set of limits that apply at the point of collapse. This system proved to be a challenging case, since all but nine outages forced a change in the limits applied at the nose.

As expected, often the change in VAR limits involved the HINP0 bus precariously close to a limit at the nominal point of collapse. In many instances, encountering this limit caused an immediate instability and this is addressed in chapter 5.

---

the flows on the outaged line appear as loads at the bus still connected to the network following the outage, and the left eigenvector components for that bus adjusted to include the components corresponding to the isolated bus. The outage estimates then correspond to the case of adding load at a bus.

Table 4.1: Non-radial Line Outages causing at least 75 MW reduction in loading margin

(nominal loading margin = 1805 MW)

Line Outage	Margin MW	Change MW (rank)	Linear MW (rank)	Quad MW(rank)	Generators at VAR Limits
29.30.1	1464	-341 (1)	-172 (1)	-266 (1)	EXET0
4.5.1	1555	-250 (2)	-82 (4)	-133 (4)	EXET0,FAWL0
7.17.1	1635	-170 (3)	-52 (9)	-87 (7)	EXET0,FAWL0,LOVE0
8.17.1	1637	-168 (4)	-54 (8)	-89 (6)	EXET0,FAWL0,LOVE0
1.7.1	1643	-162 (5)	-129 (2)	-154 (2)	EXET0,FAWL0
1.8.1	1643	-162 (6)	-129 (3)	-154 (3)	EXET0,FAWL0
11.38.1	1650	-155 (7)	-70 (5)	-101 (5)	EXET0,FAWL0,HINP0
2.4.1	1653	-152 (8)	-48 (11)	-75 (10)	EXET0,FAWL0
3.5.1	1653	-152 (9)	-51 (10)	-80 (9)	EXET0,FAWL0
11.12.1	1700	-105 (10)	-61 (6)	-83 (8)	EXET0,FAWL0,HINP0
1.3.1	1718	-87 (11)	-56 (7)	-71 (11)	EXET0,FAWL0

Table 4.2: Radial Line Outages
(nominal loading margin = 1805 MW)

Line Outage	Margin MW	Change MW (rank)	Linear MW (rank)	Quad MW(rank)	Generators at VAR Limits
18.17.1	1367	-438 (1)	-265 (1)	-366 (1)	
39.38.1	1568	-237 (2)	-167 (2)	-203 (2)	EXET0,LOVE0,HINP0
6.5.1	1738	-67 (3)	-60 (3)	-62 (3)	
20.19.1	1752	-53 (4)	-46 (4)	-57 (4)	EXET0,FAWL0,LOVE0,HINP0
22.21.1	1752	-53 (5)	-46 (5)	-57 (5)	EXET0,FAWL0,LOVE0,HINP0
13.12.1	1792	-13 (6)	-19 (6)	-20 (6)	

Table 4.3: Non-radial Line Outages causing less than 75 MW reduction in loading margin

(nominal loading margin = 1805 MW)

Line Outage	Margin MW	Change MW	Linear MW	Quad MW	Generators at VAR Limits
31.30.1	1735	-70	-33	-51	EXET0,FAWL0
9.11.1	1739	-66	-39	-51	EXET0,FAWL0,HINP0
27.19.1	**1747**	**-58**	**-6**	**-8**	EXET0,FAWL0,LOVE0,HINP0
28.21.1	**1748**	**-57**	**-5**	**-8**	EXET0,FAWL0,LOVE0,HINP0
5.7.1	1752	-53	-27	-37	EXET0,FAWL0,LOVE0
5.8.1	1755	-50	-26	-36	EXET0,FAWL0,LOVE0
10.11.1	1757	-48	-21	-29	EXET0,FAWL0,HINP0
5.10.1	1759	-46	-29	-37	EXET0,FAWL0,HINP0
16.24.1	1764	-41	-28	-39	EXET0,FAWL0,LOVE0,HINP0
16.24.2	1764	-41	-28	-39	EXET0,FAWL0,LOVE0,HINP0
12.38.1	**1767**	**-38**	**-12**	**-12**	EXET0,FAWL0,LOVE0,HINP0
12.38.2	**1767**	**-3**	**-12**	**-12**	EXET0,FAWL0,LOVE0,HINP0
17.23.1	1771	-34	-24	-29	EXET0,FAWL0,HINP0
17.23.2	1771	-34	-24	-29	EXET0,FAWL0,HINP0
26.40.2	1775	-30	-17	-27	EXET0,FAWL0,LOVE0,HINP0
26.40.1	1775	-30	-17	-27	EXET0,FAWL0,LOVE0,HINP0
37.36.1	**1777**	**-28**	**-4**	**-8**	EXET0,FAWL0,LOVE0
25.26.1	1778	-27	-17	-25	EXET0,FAWL0,LOVE0,HINP0
25.26.2	1778	-27	-17	-25	EXET0,FAWL0,LOVE0,HINP0
5.9.1	1778	-27	-12	-14	EXET0,FAWL0,HINP0
32.36.1	1779	-26	-14	-21	EXET0,FAWL0,LOVE0
16.23.1	1785	-20	-18	-23	EXET0,FAWL0,LOVE0,HINP0
16.23.2	1785	-20	-18	-23	EXET0,FAWL0,LOVE0,HINP0
12.25.1	1787	-18	-16	-22	EXET0,FAWL0,LOVE0,HINP0
12.25.2	1787	-18	-16	-22	EXET0,FAWL0,LOVE0,HINP0
31.32.1	1787	-18	-5	-8	EXET0,FAWL0,LOVE0
1.2.1	1791	-14	-14	-13	EXET0,FAWL0,LOVE0,HINP0
15.16.1	1791	-14	-7	-9	EXET0,FAWL0,LOVE0,HINP0
15.16.2	1791	-14	-7	-9	EXET0,FAWL0,LOVE0,HINP0
12.15.1	1793	-12	-14	-20	EXET0,FAWL0,LOVE0,HINP0
12.15.2	1793	-12	-14	-20	EXET0,FAWL0,LOVE0,HINP0
12.14.1	1800	-5	-4	-4	EXET0,FAWL0,LOVE0,HINP0
14.38.1	1800	-5	-2	-2	EXET0,FAWL0,LOVE0,HINP0
17.19.1	1809	4	0	2	EXET0,FAWL0,LOVE0
17.21.1	1809	4	0	2	EXET0,FAWL0,LOVE0

Chapter 5

Voltage Collapse due to VAR limits

The previous sections and the theory presented in [12, 13] associate voltage collapse of the electric power system with a fold bifurcation of the equilibrium equations used to model the system. Experience [4, 3, 10, 11, 14, 15] has shown that the VAR limitations of generators are associated with voltage instability, and computational experience shows that the effect of changing PV buses in the equilibrium model of the power system to PQ buses often reduces the loading margin to voltage collapse.

In some cases, when the system loading is high, the effect of changing a PV bus to a PQ bus causes the margin to the fold bifurcation to increase. Upon application of the limit, the equilibrium point appears on the bottom half of the nose curve, and voltages increase upon increase in load [7, 14].

The points at which changing a PV bus to a PQ bus alter the system nose curve so that the equilibrium solution is on the lower voltage branch of the new nose curve are points at which the power system becomes immediately unstable [7, 2]. We refer to these points as points of immediate instability, to distinguish them from fold bifurcation points. However, either a fold bifurcation point or point of immediate instability can lead to a dynamic voltage collapse.

Tables 5.1,5.2, and 5.3 show the same results as in chapter 4 except that the actual margins are adjusted to reflect the cases in which an immediate instability was encountered before the fold bifurcation at the nose of the curve. In all cases, the VAR limit was caused by the generator at HINP0.

Those cases for which a change in margin occurs are highlighted in bold. The immediate instability caused only minor changes in ranking between outages within 5 MW of each other. The outages are listed in the same order as in chapter 4.

For nearly half of the outages, instability was due to fold bifurcation, not immediate instability. All of the most serious outages were due to fold bifurcation. When the actual margin represents the distance to immediate instability and not to fold bifurcation, the margin to fold bifurcation is noted in parentheses. In all cases, fold bifurcation occurs within 11 MW of immediate instability. Table 5.4 compares the loading margins to fold bifurcation with the loading margins to immediate instability for each outage at which an immediate instability occurred before fold bifurcation.

Since all cases of immediate instability resulted from the generator at HINP0 hitting a VAR limit (although this did not always result in an immediate instability) it is natural to ask how the contingencies affect the loading margin to the HINP0 VAR limit, as opposed to the loading margin to the fold bifurcation. This topic is addressed in section 5.1.

5.1 Contingency ranking for voltage collapse due to VAR limits

The sensitivity computations can be easily extended to the case in which the voltage collapse is an immediate instability due to a VAR limit rather than a fold bifurcation. The derivation of the sensitivity formula in [12] required the description of a hypersurface of fold bifurcation points. The normal vector to this hypersurface is defined by the zero left eigenvector of the system Jacobian. Similarly we can construct a hypersurface in which each point corresponds to the point at which a particular generator is at a VAR limit. The normal vector to this hypersurface can then be used in the sensitivity formulas to compute the sensitivity of the margin to encountering the VAR limit.

Table 5.1: Non-radial Line Outages causing at least 75 MW reduction in loading margin

(nominal loading margin = 1805 MW)

Line Outage	Margin MW	Change MW (rank)	Linear MW (rank)	Quad MW(rank)	Generators at VAR Limits
29.30.1	1464	-341 (1)	-172 (1)	-266 (1)	EXET0
4.5.1	1555	-250 (2)	-82 (4)	-133 (4)	EXET0,FAWL0
7.17.1	1635	-170 (3)	-52 (9)	-87 (7)	EXET0,FAWL0,LOVE0
8.17.1	1637	-168 (4)	-54 (8)	-89 (6)	EXET0,FAWL0,LOVE0
1.7.1	1643	-162 (5)	-129 (2)	-154 (2)	EXET0,FAWL0
1.8.1	1643	-162 (6)	-129 (3)	-154 (3)	EXET0,FAWL0
11.38.1	1650	-155 (7)	-70 (5)	-101 (5)	EXET0,FAWL0,HINP0
2.4.1	1653	-152 (8)	-48 (11)	-75 (10)	EXET0,FAWL0
3.5.1	1653	-152 (9)	-51 (10)	-80 (9)	EXET0,FAWL0
11.12.1	**1699 (1700)**	-106 (10)	-61 (6)	-83 (8)	EXET0,FAWL0,HINP0
1.3.1	1718	-87 (11)	-56 (7)	-71 (11)	EXET0,FAWL0

Table 5.2: Radial Line Outages
(nominal loading margin = 1805 MW)

Line Outage	Margin MW	Change MW (rank)	Linear MW (rank)	Quad MW(rank)	Generators at VAR Limits
18.17.1	1367	-438 (1)	-265 (1)	-366 (1)	
39.38.1	1568	-237 (2)	-167 (2)	-203 (2)	EXET0,LOVE0,HINP0
6.5.1	1738	-67 (3)	-60 (3)	-62 (3)	
20.19.1	**1750 (1752)**	-55 (4)	-46 (4)	-57 (4)	EXET0,FAWL0,LOVE0,HINP0
22.21.1	**1750 (1752)**	-55 (5)	-46 (5)	-57 (5)	EXET0,FAWL0,LOVE0,HINP0
13.12.1	1792	-13 (6)	-19 (6)	-20 (6)	

Table 5.3: Non-radial Line Outages causing less than 75 MW reduction in loading margin

(nominal loading margin = 1805 MW)

Line Outage	Margin MW		Change MW	Linear MW	Quad MW	Generators at VAR Limits
31.30.1	1735		-70	-33	-51	EXET0,FAWL0
9.11.1	**1735**	**(1739)**	-66	-39	-51	EXET0,FAWL0,HINP0
27.19.1	**1741**	**(1747)**	-64	-6	-8	EXET0,FAWL0,LOVE0,HINP0
28.21.1	**1742**	**(1748)**	-63	-5	-8	EXET0,FAWL0,LOVE0,HINP0
5.7.1	1752		-53	-27	-37	EXET0,FAWL0,LOVE0
5.8.1	1755		-50	-26	-36	EXET0,FAWL0,LOVE0
10.11.1	**1750**	**(1757)**	-55	-21	-29	EXET0,FAWL0,HINP0
5.10.1	**1753**	**(1759)**	-52	-29	-37	EXET0,FAWL0,HINP0
16.24.1	**1757**	**(1764)**	-48	-28	-39	EXET0,FAWL0,LOVE0,HINP0
16.24.2	**1757**	**(1764)**	-48	-28	-39	EXET0,FAWL0,LOVE0,HINP0
12.38.1	**1767**	**(1767)**	-38	-12	-12	EXET0,FAWL0,LOVE0,HINP0
12.38.2	**1767**	**(1767)**	-38	-12	-12	EXET0,FAWL0,LOVE0,HINP0
17.23.1	**1769**	**(1771)**	-36	-24	-29	EXET0,FAWL0,HINP0
17.23.2	**1769**	**(1771)**	-36	-24	-29	EXET0,FAWL0,HINP0
26.40.2	**1769**	**(1775)**	-36	-17	-27	EXET0,FAWL0,LOVE0,HINP0
26.40.1	**1770**	**(1775)**	-35	-17	-27	EXET0,FAWL0,LOVE0,HINP0
37.36.1	1777		-28	-4	-8	EXET0,FAWL0,LOVE0
25.26.1	**1771**	**(1778)**	-34	-17	-25	EXET0,FAWL0,LOVE0,HINP0
25.26.2	**1771**	**(1778)**	-34	-17	-25	EXET0,FAWL0,LOVE0,HINP0
5.9.1	**1780**	**(1778)**	-29	-12	-14	EXET0,FAWL0,HINP0
32.36.1	1779		-26	-14	-21	EXET0,FAWL0,LOVE0
16.23.1	**1778**	**(1785)**	-27	-18	-23	EXET0,FAWL0,LOVE0,HINP0
16.23.2	**1778**	**(1785)**	-27	-18	-23	EXET0,FAWL0,LOVE0,HINP0
12.25.1	**1779**	**(1787)**	-26	-16	-22	EXET0,FAWL0,LOVE0,HINP0
12.25.2	**1779**	**(1787)**	-26	-16	-22	EXET0,FAWL0,LOVE0,HINP0
31.32.1	1787		-18	-5	-8	EXET0,FAWL0,LOVE0
1.2.1	1791		-14	-14	-13	EXET0,FAWL0,LOVE0,HINP0
15.16.1	1791		-14	-7	-9	EXET0,FAWL0,LOVE0,HINP0
15.16.2	1791		-14	-7	-9	EXET0,FAWL0,LOVE0,HINP0
12.15.1	**1782**	**(1793)**	-23	-14	-20	EXET0,FAWL0,LOVE0,HINP0
12.15.2	**1782**	**(1793)**	-23	-14	-20	EXET0,FAWL0,LOVE0,HINP0
12.14.1	1800		-5	-4	-4	EXET0,FAWL0,LOVE0,HINP0
14.38.1	1800		-5	-2	-2	EXET0,FAWL0,LOVE0,HINP0
17.19.1	1809		4	0	2	EXET0,FAWL0,LOVE0
17.21.1	1809		4	0	2	EXET0,FAWL0,LOVE0

Table 5.4: All line outages causing an immediate instability prior to fold bifurcation

(nominal loading margin = 1805 MW)

Line Outage	Margin to Immediate Instability (MW)	Margin to Fold bifurcation (MW)
11.12.1	1699	1700
9.11.1	1735	1739
27.19.1	1741	1747
28.21.1	1742	1748
10.11.1	1750	1757
20.19.1	1750	1752
22.21.1	1750	1752
5.10.1	1753	1759
16.24.1	1757	1764
16.24.2	1757	1764
12.38.1	1767	1767
12.38.2	1767	1767
17.23.1	1769	1771
17.23.2	1769	1771
26.40.2	1769	1775
26.40.1	1770	1775
25.26.1	1771	1778
25.26.2	1771	1778
5.9.1	1778	1780
16.23.1	1778	1785
16.23.2	1778	1785
12.25.1	1779	1787
12.25.2	1779	1787
12.15.1	1782	1793
12.15.2	1782	1793

Computation of nominal point of instability

Computation of the point of immediate instability is similar to computation of a fold bifurcation point. The same continuation method can be used, and the point of collapse is the point at which a VAR limit is encountered and upon further increase in load the system voltages increase. Thus, the immediate instability can be detected by computing the sensitivity of the bus voltages to the loading factor after application of the limit. (Note that the software described in [14] performs this check to detect voltage collapse due to fold bifurcation or immediate instability.)

For this study, the maximum VAR limit at HINP0 was changed from 660 MVAR to 630 MVAR. The continuation program was run as before, and again, VAR limits were reached at EXET0, FAWL0, and LOVE0. However, at a loading 5379 MW, HINP0 reaches its VAR limit of 630 MVARS, and the system becomes unstable once the PV bus is converted to a PQ bus. (A fold bifurcation of the post limit system occurs at 5385 MW. Note that the point of collapse for the original system occurred at a loading of 5380 MW due to fold bifurcation.)

Computation of sensitivity

When the voltage collapse is identified with the fold bifurcation of the equilibrium model, the left zero eigenvector can be used to compute the normal vector to the surface of bifurcation points in parameter space. Similarly, when the voltage collapse is identified with the immediate instability due to application of a VAR limit, there is a normal vector in parameter space to the surface of points at which the critical Q limit is reached. Table 5.5 compares the normal vector W to the zero left eigenvector N. The angle between N and W is 4.6 degrees. When the sensitivity computations and contingency rankings were repeated using W in place of N, no significant changes were observed.

Table 5.5: VAR normal vector W and left eigenvector N

Bus No.	Bus Name	Real Power W	N	Reactive Power W	N
1	INDQ4	0.1172	0.1357	0.3041	0.3351
2	LAND4	0.1227	0.1417	0.2936	0.3253
3	ABHA4T	0.0899	0.1061	0.224	0.2555
4	ABHA4U	0.0984	0.1153	0.2386	0.2703
5	EXET4	0.0683	0.0819	0.171	0.2018
6	EXET0	0.0683	0.0819	0.153	0.1806
7	TAUN4J	0.0552	0.0674	0.1439	0.1769
8	TAUN4K	0.0568	0.0693	0.1445	0.1776
9	AXMI4	0.0625	0.0749	0.1545	0.1826
10	CHIC4	0.0522	0.0627	0.1337	0.1584
11	MANN4	0.0404	0.0486	0.1056	0.1257
12	LOVE4	0.0206	0.0249	0.0542	0.0655
13	LOVE0	0.0206	0.0249	0.0491	0.0594
14	NURS4	0.0207	0.025	0.0593	0.0715
15	FLEE4	0.0238	0.0287	0.0373	0.0462
16	BRLE4	0.0242	0.0293	0.0307	0.0387
17	HINP4	0.0421	0.0522	0.1031	0.1376
18	HINP0	0.0281	0.0268	0	0.0608
19	HINP2J	0.045	0.0552	0.0916	0.1197
20	HINP0J	0.0258	0.0301	0	0
21	HINP2K	0.0449	0.0551	0.0915	0.1196
22	HINP0K	0.0257	0.03	0	0
23	MELK4	0.0341	0.0419	0.0651	0.0857
24	DIDC4	0.0221	0.0266	0	0
25	BOLN4	0.0094	0.0114	0.0337	0.0408
26	NINF4	0.0027	0.0033	0.0157	0.019
27	BRWA2Q	0.0502	0.0615	0.0967	0.1256
28	BRWA2R	0.05	0.0613	0.0966	0.1254
29	INDQ1	0.9086	0.9176	1	1
30	LAND1	0.3177	0.3473	0.482	0.5128
31	ABHA1	0.2107	0.2394	0.3091	0.3449
32	EXET1	0.173	0.2002	0.2479	0.2835
33	CHIC1	0.066	0.0789	0.1364	0.1615
34	MANN1	0.0988	0.1176	0.1357	0.1611
35	AXMI1	0.0955	0.1137	0.167	0.1971
36	TAUN1	0.1122	0.1355	0.1572	0.191
37	BRWA1	0.1085	0.1323	0.1385	0.1713
38	FAWL4	0.0198	0.0239	0.0617	0.0743
39	FAWL0	0.0048	0.0059	0.0597	0.0719
40	DUNG4	0	0	0	0

Appendix A

Derivation of VAR Limit Sensitivity Formulas

This appendix derives the sensitivity of the margin to a immediate instability caused by a VAR limit. The derivation is similar to that in [12] and consulting [12] first may be helpful.

Assume that (z_0, λ_0) is the present stable operating point, and that the continuation program determines that for a forecast parameter change in the direction $\hat{k}$, at the point (z_*, λ_*) a critical VAR limit is reached. The security margin is $M = \|\lambda_* - \lambda_0\|$. The equilibrium equations valid at (z_*, λ_*) are $F(z, \lambda)$. $E(z, \lambda)$ are the critical event equations at (z_*, λ_*). That is, $E(z, \lambda) = 0$ is the condition for the VAR limit to be encountered. At the nominal critical event $\begin{pmatrix} F|_{(z_*, \lambda_*, p_0)} \\ E|_{(z_*, \lambda_*, p_0)} \end{pmatrix} = 0$. The boundary that we wish to estimate is a subset of the set $E^{-1}(0) \cap F^{-1}(0)$, the set of equilibria that satisfy the VAR limit being reached in state and parameter space around the nominal point (z_*, λ_*, u_*).

Consider a curve parameterized by p, $(Z(p), \Lambda(p))$ on $E^{-1}(0) \cap F^{-1}(0)$ and passing through the point (z_*, λ_*, p_0)

$$\begin{pmatrix} F(Z(p), \Lambda(p), p) \\ E(Z(p), \Lambda(p), p) \end{pmatrix} = 0 \tag{A.1}$$

where $\Lambda(p) = \lambda_* + L(p)\hat{k}_*$ and $L(p)$ is the load change in the $\hat{k}_*$ direction as a function of p. Since $\hat{k}_*$ is a unit vector in the norm used for the margin,

the margin as a function of p is $M(p) = M|_{p_0} + L(p)$ and the sensitivity of the margin with respect to p is $M_p = L_p$. Differentiating (A.1) at (z_*, λ_*) with respect to p yields a linear system

$$\left. \begin{pmatrix} F_z & F_\lambda \hat{k}_* \\ E_z & E_\lambda \hat{k}_* \end{pmatrix} \right|_{(z_*, \lambda_*, p_0)} \begin{pmatrix} Z_p \\ L_p \end{pmatrix} = - \left. \begin{pmatrix} F_p \\ E_p \end{pmatrix} \right|_{(z_*, \lambda_*, p_0)} \tag{A.2}$$

By the inverse function theorem, if $\left. \begin{pmatrix} F_z & F_\lambda \hat{k}_* \\ E_z & E_\lambda \hat{k}_* \end{pmatrix} \right|_{(z_*, \lambda_*, p_0)}$ is nonsingular, the map $(Z(p), \Lambda(p))$ is bijective in a neighborhood about (z_*, λ_*, p_0). The sensitivities can then be computed. Solution of (A.2) yields:

- Z_p, the tangent vector at (z_*, λ_*, p_0) to the curve in state space that describes how the state variables change to satisfy the equilibrium and event conditions as p varies[1]. $Z_p \Delta p$ is the first order Taylor series estimate of how the state changes on $E^{-1}(0) \cap F^{-1}(0)$ for a parameter change of Δp.

- L_p (a scalar), the sensitivity with respect to p of the load change in the $\hat{k}_*$ direction.

The first order estimate of the change in margin corresponding to the change in p of Δp is

$$\Delta M = L_p \Delta p \tag{A.3}$$

Since the matrix $\left. \begin{pmatrix} F_z & F_\lambda \hat{k}_* \\ E_z & E_\lambda \hat{k}_* \end{pmatrix} \right|_{(z_*, \lambda_*, p_0)}$ is the same for any[2] parameter p, once the matrix is factored and the sensitivities obtained for one parameter, computing the sensitivities for any additional parameters only requires obtaining the derivatives $\left. \begin{pmatrix} F_p \\ E_p \end{pmatrix} \right|_{(z_*, \lambda_*, p_0)}$ and one forward and backward substitution.

---

[1]thus $Z_p \Delta p$ can be used to screen for cases where new limits would be violated ($Z_p \Delta p[i] > Z_{lim}[i]$)

[2]The presentation assumes that $\hat{k}$ does not explicitly depend on p and that p is not a component of λ. The appropriate formulas for these special cases are simply obtained by applying the chain rule for derivatives similarly to the appendix in [12].

If obtaining M_p for many parameters is of primary interest, and there is no desire to obtain Z_p, then full solution of the linear system (A.2) is not necessary. The matrix $\left(\begin{array}{c} F_z \\ E_z \end{array} \right)\Big|_{(z_*,\lambda_*,p_0)}$ has n columns and $n+1$ rows. Since every set of $n+1$ vectors in $\mathbf{R}^n$ is linearly dependent there is a nonzero vector w such that

$$w \left(\begin{array}{c} F_z \\ E_z \end{array} \right)\Bigg|_{(z_*,\lambda_*,p_0)} = 0 \tag{A.4}$$

w^T is a vector in the null space of $(F_z^T, E_z^T)|_{(z_*,\lambda_*,p_0)}$ and can be found with less computational expense than required for solution of equation (A.2). If $\left(\begin{array}{c} F_z \\ E_z \end{array} \right)\Big|_{(z_*,\lambda_*,p_0)}$ has full rank then w is unique up to a scalar multiplication. Premultiplying (A.2) by w yields

$$L_p = - \frac{w \left(\begin{array}{c} F_p \\ E_p \end{array} \right)\Bigg|_{(z_*,\lambda_*,p_0)}}{w \left(\begin{array}{c} F_\lambda \hat{k} \\ E_\lambda \hat{k} \end{array} \right)\Bigg|_{(z_*,\lambda_*,p_0)}} \tag{A.5}$$

Note that regardless of the number of parameters under consideration, w needs to be computed only once.

Bibliography

[1] C.A. Cañizares, F.L. Alvarado, "Point of collapse and continuation methods for large AC/DC systems", *IEEE Trans. Power Systems*, vol.7, no.1, Feb.1993, pp.1-8.

[2] M.L. Crow, J. Ayyagari, "The effect of excitation limits on voltage stability", *IEEE Trans. Circuits and Systems — I:Fundamental Theory and Applications*, vol. 42, no. 12, December 1995.

[3] L.H. Fink, ed., Proceedings: Bulk power system voltage phenomena III, voltage stability, security & control, ECC/NSF workshop, Davos, Switzerland, August 1994.

[4] L.H. Fink, ed., Proceedings: Bulk power system voltage phenomena, voltage stability and security, ECC/NSF workshop, Deep Creek Lake, MD, Aug. 1991, ECC Inc., 4400 Fair Lakes Court, Fairfax, VA 22033-3899.

[5] I. Dobson, H.-D. Chiang, "Towards a theory of voltage collapse in electric power systems, *Systems and Control Letters*, vol. 13, 1989, pp. 253-262.

[6] I. Dobson, L. Lu, "Computing an optimum direction in control space to avoid saddle node bifurcation and voltage collapse in electric power systems", *IEEE Trans. Automatic Control*, vol 37, no. 10, October 1992, pp. 1616-1620.

[7] I. Dobson, L. Lu, "Voltage collapse precipitated by the immediate change in stability when generator reactive power limits are encountered", *IEEE Trans. Circuits and Systems, Part 1*, vol. 39, no. 9, Sept. 1992, pp. 762-766.

[8] G.C. Ejebe, H.P. Van Meeteren, B.F. Wollenberg, "Fast contingency screening and evaluation for voltage security analysis", *IEEE Trans. Power Systems*, vol. 3, no. 4, November 1988, pp. 1582-1590.

[9] G.C. Ejebe, G.D. Irisarri, S. Mokhtari, O. Obadina, P. Ristanovic, J. Tong, "Methods for contingency screening and ranking for voltage stability analysis of power systems", *IEEE Trans. Power Systems*, vol. 11, no. 1, February 1996, pp. 350-356.

[10] N. Flatabø, R. Ognedal, T. Carlsen, "Voltage stability condition in a power transmission system calculated by sensitivity methods", *IEEE Trans. Power Systems*, vol. 5, no. 4, November 1990, pp. 1286-1293.

[11] N. Flatabø, O.B. Fosso, R. Ognedal, T. Carlsen, K.R. Heggland, "A method for calculation of margins to voltage instability applied on the Norwegian system for maintaining required security level", *IEEE Trans. Power Systems*, vol. 8, no. 2, May 1993, pp. 920-928.

[12] S. Greene, I. Dobson, F.L. Alvarado, "Sensitivity of the loading margin to voltage collapse with respect to arbitrary parameters", *IEEE Trans. Power Systems*, vol. 12, no. 1, February 1997, pp. 262-272.

[13] S. Greene, I. Dobson, F.L. Alvarado, "Contingency ranking for voltage collapse via sensitivities from a single nose curve", paper SM97-707, presented at the IEEE PES Summer Meeting, Berlin, Germany, July 1997

[14] N. T. Hawkins, G. Shackshaft, M.J. Short, "On-line algorithms for the avoidance of voltage collapse: reactive power management and voltage collapse margin assessment", Third International Conference on Power System Monitoring and Control, Institution of Electrical Engineers, London, UK

[15] N. T. Hawkins "On-line reactive power management in electric power systems", PhD thesis, University of London, Department of Electrical and Electronic Engineering, Imperial College of Science, Technology, and Medicine, London, UK

[16] T. Van Cutsem, "An approach to corrective control of voltage instability using simulation and sensitivity", Proceedings Athens Power Tech 1993, Athens, Greece, September 5-8, 1993.